의학박사 학위논문

ST2 차단이 사구체 족세포 손상과 세뇨관-간질 섬유화에 미치는 영향에 대한 연구

ST2 blockade abrogates podocyte injury and tubulo-interstitial fibrosis

2019년 2월

서울대학교 의학대학원

임상약리학과 협동과정

김 용 철

의학박사 학위논문

ST2 차단이 사구체 족세포 손상과 세뇨관-간질 섬유화에 미치는 영향에 대한 연구

ST2 blockade abrogates podocyte injury and tubulo-interstitial fibrosis

2019년 2월

서울대학교 의학대학원

임상약리학과 협동과정

김 용 철

ST2 차단이 사구체 족세포 손상과 세뇨관-간질 섬유화에 미치는 영향에 대한 연구

ST2 blockade abrogates podocyte injury and tubulo-interstitial fibrosis

지도교수 장 인 진

이 논문을 의학박사 학위논문으로 제출함

2018년 10월

서울대학교 대학원

임상약리학과 협동과정

김 용 철

김용철의 의학박사 학위논문을 인준함

2019년 1월

위 원 장 김 연 수 (인)

부 위 원 장 장 인 진 (인)

위 원 주 권 욱 (인)

위 원 조 주 연 (인)

위 원 박 철 휘 (인)

Abstract

ST2 blockade abrogates podocyte injury and tubulo-interstitial fibrosis

Yong Chul Kim
Medicine, Clinical Pharmacology
The Graduate School
Seoul National University

Suppression of tumorigenicity 2 (ST2) which is the receptor of IL-33 is involved in renal inflammation and it is also correlated with disease severity in chronic kidney disease (CKD). Here, we report the ameliorating effect of the ST2 blockade as well as the role of ST2 in the progression of renal fibrosis.

Serum and urine levels of soluble ST2 (sST2) were measured in 296 CKD patients. And ST2 mRNA levels were quantified in blood and urine cells. Immunohistochemistry (IHC) stain of ST2 was performed in kidney biopsy samples of CKD patients. Further, urine cells were co-stained with podocalyxin/aquaporin-1 and ST2 to characterize the cell type. And fibrosis induced by TGF-β in primary cultured podocytes and proximal tubular epithelial cells (PTECs) were evaluated with fibronectin and ST2 mRNA expressions. Anti-ST2 monoclonal antibody (mAb) was treated to evaluate the

neutralizing effect of ST2 on renal fibrosis. Finally, ST2 and fibronectin mRNA expression was measured in CKD mouse model (UUO; Unilateral Ureteral Obstruction).

Serum ($P = 0.002$) and urine ($P < 0.001$) sST2 levels increased as renal function deteriorated. Also, urine ST2 levels adjusted by urine creatinine showed the same pattern ($P < 0.001$). Serum ($P = 0.023$) and urine ($P = 0.03$) ST2 expressions were elevated in CKD stage 5 patients compared with other stages. ST2 IHC staining in CKD stage 5 showed 3-fold increase than CKD stage 1. When the patients were subdivided by 0.5 g/g proteinuria, patients with more proteinuria had a higher concentration of urine ST2 ($P = 0.02$). A large portion of urine cells were ST2-rich podocytes/PTECs and the proportion of these cells increased as renal function decreased in flow-cytometry. After fibrosis induction in primary cultured podocytes and PTECs, mRNA and protein expressions of fibronectin and ST2 showed positive correlation with the fibrosis severity. And anti-ST2 blocking Ab neutralized the fibrosis. In UUO mouse model, ST2 and fibronectin expression increased over time ($P < 0.01$).

Elevated serum and urine ST2 levels are associated with the progression of CKD and podocytes/PTECs are involved in this process. ST2-mediated signaling may have a considerable role in the progression renal dysfunction. And ST2 blockade is a potential therapeutic target for renal preservation.

.....

Keywords: ST2, podocyte, proximal tubular epithelial cell, chronic kidney disease, renal fibrosis

Student Number: 2010-21888

Contents

List of tables and figures

INTRODUCTION

The prevalence of CKD is gradually increasing worldwide, CKD is a major burden to the health care system in terms of not only cost, but also co-morbidity and mortality.(1)

Renal fibrosis, characterized by glomerulosclerosis (GS) and tubulointerstitial fibrosis (TIF), is a common pathological outcome of CKD, regardless of etiology.(2-4) Progressive CKD often results in excessive accumulation of extracellular matrix that leads to the complete destruction of kidney and end-stage renal failure that requires dialysis or kidney transplantation.(5)

Renal fibrosis represents a failed wound-healing process of the kidney tissue after chronic, sustained injury. Among many kinds of fibrogenic factors that regulate renal fibrotic process, transforming growth factor-β (TGF-β) is one that plays a central role. TGF-β can stimulate mesangial cells, interstitial fibroblasts, and tubular epithelial cells to undergo myofibroblastic activation or transition, to become matrix-producing fibrogenic

cells. The hyperfiltration theory of Brenner *et al.*, which suggests that the progression of renal disease results from glomerular hemodynamic changes, has been emerged as a popular concept. However, close pathologic analysis recently showed that functional impairment of the kidney is better correlated with the degree of tubule-interstitial damage than with that of glomerular injury, and this finding in turn has led to the broad recognition that the final common pathway of kidney failure operates principally in the tubule-interstitium. Nevertheless, several reports have shown that podocyte play a key role in glomerulosclerosis which results in renal fibrosis by interacting with other kidney cells such as mesangial cells, endothelial cells and tubular epithelial cells.(6-8)

Suppression of tumorigenicity 2 (ST2) is an interleukin (IL)-1 receptor family member which exists as soluble (sST2) and trans-membrane isoform. Interleukin-33 is the functional ligand of ST2 which is known to play an active role in inflammation and fibrosis in various organs.(9-11)

sST2 elevation in kidney diseases has been described in limited studies, such as lupus nephritis, renal transplantation and a small cohort of CKD patients. Elevated serum sST2 level in Systemic lupus erythematosus (SLE) patients was found to correlate with disease activity and was sensitive to change, suggesting a potential role as a surrogate marker of disease activity.(12) Thierry et al. reported that serum and urine IL-33/sST2 levels were significantly elevated as soon as 30 min after reperfusion during kidney transplantation, showing a potential role of IL-33 and sST2 as an innate-immune mediator during kidney ischemia-reperfusion injury (IRI) in humans.(13)

Elevated concentration of serum sST2 is found in CKD patients and correlates with renal functions.(14) Although the serum sST2 level has previously been found to be correlated in patients with CKD, its causal relationship remains unclear. Furthermore, the urine level of sST2 has also not been described in CKD patients before.

The role of ST2 has not previously been described in renal

fibrosis.(14) On this background, this study aims to examine serum and urine levels of sST2 in patients with CKD and to explore their association with renal fibrosis.

METHODS

Study Population

Details of patients and controls are summarized in Table 1. We recruited Chronic Kidney Disease (CKD) patients who were attending the Seoul National University and the Seoul K internal medicine clinic. We also recruited healthy subjects. In total, samples from 295 CKD patients were included.

Measurement of serum and urine ST2

The sST2 ELISA (catalog no. M3300) kit was obtained from R&D Systems, Inc (Minneapolis, MN). ELISA was performed according to the manufacturer' s instructions. The lower limit of detection for sST2 was 31.3 pg/ml.

Histologic Examination

Paraformaldehyde (4%)-fixed and paraffin-embedded kidneys were sectioned at 4 _m and stained with periodic acid-Schiff (PAS) by standard methods. All histologic examinations were performed by the renal pathologist in a blinded fashion. Histopathological changes were individually scored by two independent investigators.

Sections were deparaffinized in xylene and rehydrated in a

graded series of ethanol. Endogenous peroxidase activity was blocked with 0.3% hydrogen peroxidase in methanol for 30 min at room temperature. Sections were microwaved for 5 min to retrieve the antigen in an antigen unmasking solution. After incubation with 5% skim milk for 1 h at room temperature, sections were incubated at 4° C with a primary mouse monoclonal anti-ST2L antibody and anti-podocalyxin overnight. Tissues were washed several times in PBS and incubated for 45 min with a secondary antibody. Tissues were visualized using a DAB or AEC kit, examined under a microscope and photographed.

Urine sample collection and RNA extraction

Whole stream early morning urine specimens were collected from each study participant, and samples were centrifuged at 2,000 *g* for 10 min at 4° C. The urinary supernatant was discarded, and the remaining cell pellets were resuspended in 1.5 ml DEPC-treated PBS and centrifuged at 13,000 *g* for 5 min at 4° C. The pellets were resuspended in 1.0 ml TRIzol Reagent (Ambion, Life Technologies) and stored at − 80° C until use.

Real-time quantitative PCR analysis

Total RNA was extracted from podocytes/PTECs and the mRNA levels of target genes were assayed by real-time quantitative PCR. Briefly, total RNA was isolated from podocytes/PTECs using the RNeasy kit (Qiagen GmBH, Germany), and 500 ng of total RNA was reverse-transcribed using oligo-d(T) primers and AMV-RT Taq polymerase (Promega, WI, USA). Real-time qPCR was performed using Assay-on-Demand TaqMan probes and primers for NGAL, IL-8, fibronectin, collagen1, αSMA and GAPDH (Applied Biosystems, CA, USA) and an ABI PRISM 7500 sequence detection system. Relative quantification was performed using the $2^{-\Delta\Delta CT}$ method. GAPDH was used as a loading control. All experiments were completed in triplicate.

Western blot analysis

The podocytes/PTECs were harvested from culture plates and proteins were extracted using RIPA buffer containing Halt protease inhibitor (Pierce, IL, USA). Western immunoblotting was performed using primary antibodies against fibronectin (Santa Cruz Biotechnology, Dallas, TX), ST2 (Santa Cruz Biotechnology), and β-actin (Sigma-Aldrich). Briefly, equal amounts (30 μg) of extracted protein were separated by 10% SDS-polyacrylamide gels and transferred onto Immobilon-FL 0.4 μM polyvinylidene difluoride membranes (Millipore, MA, USA). Anti-rabbit IgG (Cell Signaling Technology, MA, USA) and anti-mouse IgG (Cell Signaling Technology) were used as

HRP-conjugated secondary antibodies. Labeled proteins were detected using an enhanced chemiluminescence system (ECLTM PRN 2106; Amersham Pharmacia Biotech, Buckinghamshire, UK), and the intensities of the bands were analyzed using a gel documentation system (Bio-Rad Gel Doc 1000 and Multi-Analyst□version 1.1).

Confocal microscopic examination

The microfluidics devices were disassembled for immunofluorescence staining, and the cells on the PDMS slabs were washed with PBS and fixed in 4% paraformaldehyde for 20 minutes. Following fixation, the cells were permeabilized with 0.3% Triton X and stained with antibodies against ST2 (Santa Cruz Biotechnology), podycalyxin, and aquaporin-1 in a blocking agent overnight at 4° C. Alexa 488/555-conjugated probes (Molecular Probes, OR, USA) were used as secondary antibodies and 4',6-diamidino-2-phenylindole (DAPI; Molecular Probes) was used to counterstain the nuclei. The primary antibodies were omitted in the negative controls. After stimulation, Z-sectioned fluorescent images were used to determine the localization of podocalyxin/aquaporin-1 in the podocytes/PTECs, respectively. Immunofluorescence images were acquired with a confocal microscope (Leica TCS SP8, Leica Microsystem GmbH Wetzlar, Germany) and were analyzed with Leica IMARIS 7.6.

Fluorescence-activated cell sorting (FACS) analysis

FACS analysis was performed using a FACS BD Calibur instrument to verify that the ST2 Ab could bind cMet. podocytes/PTECs were used. Cells were cultured using F12 HAMS media supplemented with 10% FBS (Gibco), 1% P/X, 2% HEPES and EGM (Lonza, CC-3124). For the experiment, podocytes/PTECs cells (5×10^5) were added to a 1.5ml tube, and the culture was washed out. Then, 4 ㎕ of ST2 Ab was diluted in 100 ㎕ of PBS, after which this solution was reacted with the cell suspension at 4° C for 30 minutes. Afterward, the cells were centrifuged at 4000 rpm for 3 minutes and washed twice. Then, 2 ㎕ of anti-human IgG-PE (Southern Biotech) was added to the suspension, and the cells were washed, resuspended in 1 ml of PBS, and then subjected to FACS analysis.

Podocytes in Culture/Proximal Tubular Epithelial Cells in Culture

The schematic experimental procedure is presented in Fig. 1. Human primary podocytes were harvested as previously reported.(15) Surgically resected kidney specimens were obtained from patients diagnosed with renal cell carcinoma, and the kidney cortices were dissected mechanically. The glomeruli were isolated by sieving techniques, and the isolated glomeruli were cultured for 8 days. The outgrowing cells were trypsinized

and passed through sieves with a 25-□m pore size to remove the remaining glomerular cores, which primarily consisted of mesangial cells.(16) To quantitatively analyze the podocyte from the isolated glomeruli, flow cytometry analysis was conducted. On day 8, the cultured cells were enumerated, and 1 × 10^6cells were incubated with Fc receptor blocking reagent (1㎍/ml, BDBioscience, CA, USA). Podocyte were identified using rabbit anti-human purified anti-Nephrin (Abcam,Cambridge,UK) and FITC-labeled anti-rabbit IgG (BDPharMingen, CA, USA). We isolated PTECs from normal adjacent kidney tissue specimens from patients with renal cell carcinoma according to guidelines approved by the Institutional Review Board of Seoul National University Hospital (IRB no. 1404-117-515). After dissecting the cortex, the unaffected specimens were minced and digested with Hank's balanced salt solution (HBSS) containing 3 mg/mL collagenase (Sigma-Aldrich, St. Louis, MO, USA). After centrifugation for 5 minutes at 500 g, cortical tubular cells were isolated. The cells were then incubated in DMEM/F12. After 4 hours of incubation, the tubules were collected and cultured on collagen-coated petri dishes (BD Biosciences, Franklin Lakes, NJ, USA) until colonies of epithelial cells were established, and 2±3 passages were used in the current study. After 3 days of culture, the cells were detached from the dishes with a 3 mM EDTA solution and a minimal amount of trypsin. Cells (2 × 10^5/well) were seeded on 8-well chamber slides in serum-free

medium for 24 hours and then was hed twice with PBS. Next, recombinant TGFβ (R&D Systems, Minneapolis, MN, USA) was added (final concentration, 10ng/ml) except where indicated.

Fibrosis induction and ST2 blocking Antibody Administration

Renal fibrosis was induced in primary cultured podocytes and PTECs with 2ng/ml of recombinant TGF- β. The anti-ST2 mAb was from Centocor, a pharmaceutical company of Johnson & Johnson (CNT03914). Primary cultured podocytes and PTECs were treated simultaneously with rTGF-β and 0.25 mcg/ml of anti-ST2 mAb. The doses of anti-ST2 mAg were increased to 0.5 and 1.0 mcg/ml, sequentially.

Annexin V/propidium iodide staining assay

Cell apoptosis and necrosis were measured using an Annexin V/propidium iodide (PI) fluorescein isothiocyanate (FITC) apoptosis kit (BD, Franklin Lakes, NJ, USA) by flow cytometry according to the manufacturer's instructions.(17-19) Briefly, harvested cells (5×10^5)were washed with cold PBS, resuspended in 100μL of binding buffer, stained with 5μL of FITC-conjugated Annexin V (10mg/mL) and 10μL of PI (50mg/mL), and incubated for 30 minutes at room temperature in the dark. Then, the data were acquired and analyzed with

BDFACSDiva^{TM}(V8.0, BDBiosciences, Becton, Dickinson and Company, CA, USA).

Statistical analysis

The results were expressed as the means ± SD or means ± SEM where indicated. Statistical analysis was performed using GraphPad Prism 5.0 (Graph Pad Software, CA, USA). A *P*-value <0.05 was considered statistically significant.

Ethics statement

The study protocol complies with the Declaration of Helsinki and received full approval from the institutional review board at the Seoul National University Hospital (No. H-1701-133-829). All the samples were immediately recruited, stored and monitored by the SNUH Human Biobank.

RESULTS

Clinical characteristics of CKD patients

The total number of patients enrolled in this study was 296. The baseline characteristics of CKD patients are shown in Table 1. The average age was 55.7 years old and 59.5% were male. Serum creatinine was 2.28 ± 1.88 and estimated glomerular filtration rate (GFR) was 50.2 ± 32.8 which was calculated by the Modification of Diet in Renal Disease (MDRD) GFR equation. Random urine protein creatinine ratio was 1.34 ± 2.58 g/g.

Serum and urine sST2 in CKD patients

Serum sST2, measured by enzyme-linked immunosorbent assay (ELISA), was significantly increased in patients with CKD stage V compared with CKD I, II, III, and IV ($P<0.05$). And also increased in CKD IV compared with CKD I, II, and III ($P<0.05$). Urine sST2 level had a similar pattern with serum sST2, and this trend unchanged after sST2 was divided by urine creatinine (Figure 1A). These data suggest that sST2 increases systemically and locally as kidney function deteriorates supporting a key role of ST2 in the progression of renal fibrosis.

Immunohistochemistry for ST2L in kidney specimens of CKD patients

Table 1. Baseline characteristics of CKD pateints.

CKD stage	Total	1	2	3	4	5
Number of patients, n (%)	296	42	60	87	53	54
Age (years)	55.7 ± 15.7	40.0 ±14.6	52.1±14.3	58.7 ±14.6	60.4 ±14.6	62.5 ±11.4
Male patients (%)	59.5	35.7	65.0	69.0	66.0	50.0
Blood hemoglobin (d/gl)	12.7 ± 2.1	13.7 ±1.5	14.3 ±1.6	13.3 ±1.8	11.5 ±1.4	10.4 ±1.3
White blood cell (/ul)	6746 ± 2189	6406±255	6290±2012	7010±2144	7239±1853	6605±236
Serum		5				9
uric acid (mg/dl)	6.20 ± 1.61		5.86±1.31	6.50±1.49	6.56±1.76	
Cholesterol (mg/dl)	179.2 ± 42.5	5.27±1.40	193.7±42.3	183.8±44.4	171.6±40.2	6.39±1.80
Albumin (g/dl)	4.19 ± 0.44	180.8±35.2	4.41±0.37	4.18±0.41	4.02±0.47	162.3±41.0
Bilirubin (mg/dl)	0.77 ± 0.60	4.40±0.29	1.05±0.94	0.88±0.63	0.57±0.18	3.99±0.45
AST (U/L)	23.8 ± 13.3	0.78±0.39	27.1±21.2	24.1±9.1	21.3±6.7	0.47±0.19
ALT (U/L)	24.9 ± 27.2	25.5±15.8	31.5±47.5	27.8±24.3	19.5±10.1	20.7±9.2
urea (mg/dl)	31.8 ± 22.8	25.7±20.6	15.6±4.5	24.7±7.5	43.4±12.6	17.6±8.3
Creatinine (mg/dl)	2.28 ± 1.88	12.4±4.2	1.01±0.16	1.54±0.35	2.86±0.70	64.7±26.5
eGFR (ml/min.1.73m^2)	50.2 ± 32.8	0.77±0.12	77.6±6.6	46.0±8.7	22.4±4.3	5.48±1.93
Urine Protein/Creatinine ratio	1.34 ± 2.58	105.9±9.7	0.27±0.87	1.02±1.33	2.15±3.48	10.5±3.1
Cause of CKD (%)		0.09±0.12				3.51±3.92
Diabetes	12.5		4.3	10.9	10.3	
Hypertension	6.3	0	8.7	5.5	12.8	28.2
Glomerulonephritis	26.7	0	34.8	32.7	33.3	2.6
Others	54.5	20.0	52.2	50.9	53.8	10.3
		80.0				58.9

Data are presented as mean (SEM) or frequencies (percentage). Abbreviations: CKD, chronic kidney disease; AST; aspartate transaminase, ALT; alanine transaminase, eGFR, estimated glomerular filtration rate.

Immunofluorescence and confocal imaging for ST2L in the kidney of CKD patients was performed. ST2L was clearly seen in glomeruli and also in (proximal) tubular epithelial cells (Figure 1B, 1C). To determine whether the ST2L staining in the glomeruli area was in podocyte, podocalyxin was performed. There was an increasing tendency of ST2L staining as kidney function deteriorates.

Increased expression of ST2L in whole blood cells and urine sediment cells

Increased ST2L mRNA transcripts were measured in whole blood cells in CKD 5 patients compared with CKD 2 ($P < 0.05$), 3 ($P < 0.01$), 4 ($P < 0.05$). IL-8 was also up-regulated in whole blood cells in CKD 5 compared with CKD 3 ($P < 0.05$). ST2L mRNA expression was increased in urine sediment cells in CKD 5 patients compared with CKD 2, 3, and 4 ($P<0.05$). But, there was no difference in the expression of NGAL mRNA (Fugure 1D). Taken together, these data indicated that increased expression of ST2L mRNA in whole blood and urine sediment cells was consistent with our previous results demonstrating overall elevated sST2 levels in serum and urine of CKD patients.

Correlation of serum and urine sST2 and proteinuria in CKD patients

When patients were divided into two groups according to 0.5

g/g of proteinuria, urine sST2 and urine sST/Cr levels were significantly increased in patients with proteinuria more than 0.5 g/g ($P < 0.05$). There was no difference in serum sST2 between two groups (Figure 1E). As increasing proteinuria is mainly related with dysfunction of the podocytes, we hypothesized that podocyte might play an important role in the progression of CKD and the development of kidney fibrosis.

Figure 1. ST2 in CKD patients

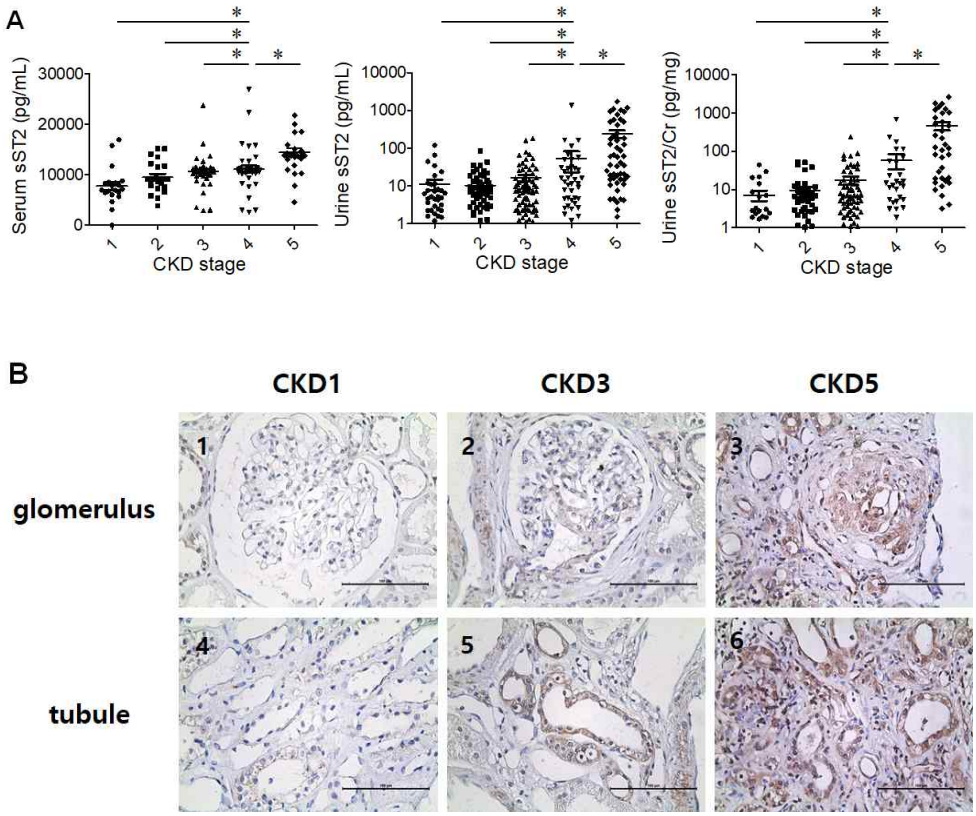

(A) sST2 concentrations in plasma and urine from CKD patients. (B) Representative images of ST2L staning in glomerulus (panel 1, 2, 3) and tubulo-interstitium (4, 5, 6) from CKD patients. Original magnification: X 400. Scale bar 100 um.

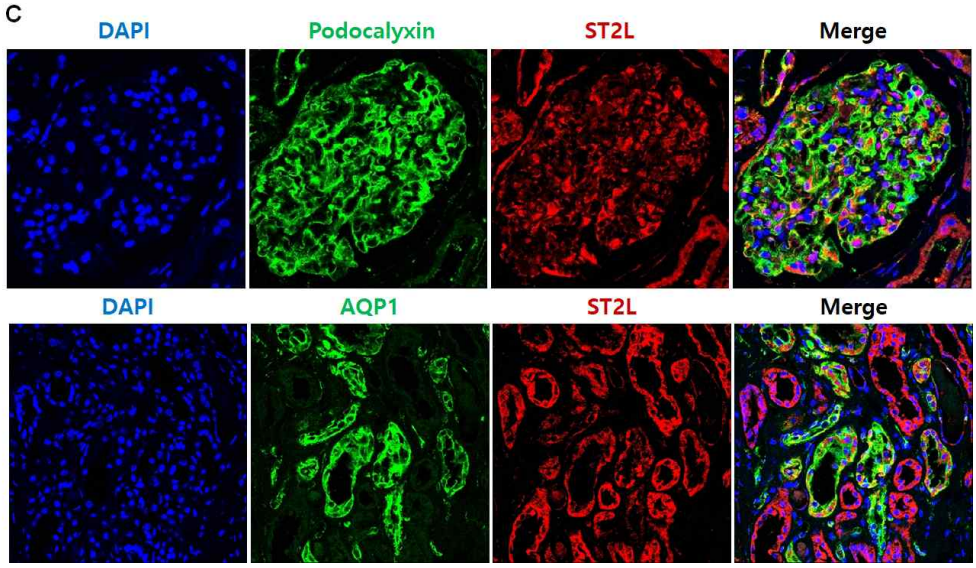

(C) Representative confocal microscopic images of human kidney biopsy samples in CKD 5 patients co-stained for ST2L (red), podocalyxin/aquaporin-1 (green) and DAPI (blue). Original magnification: X400.

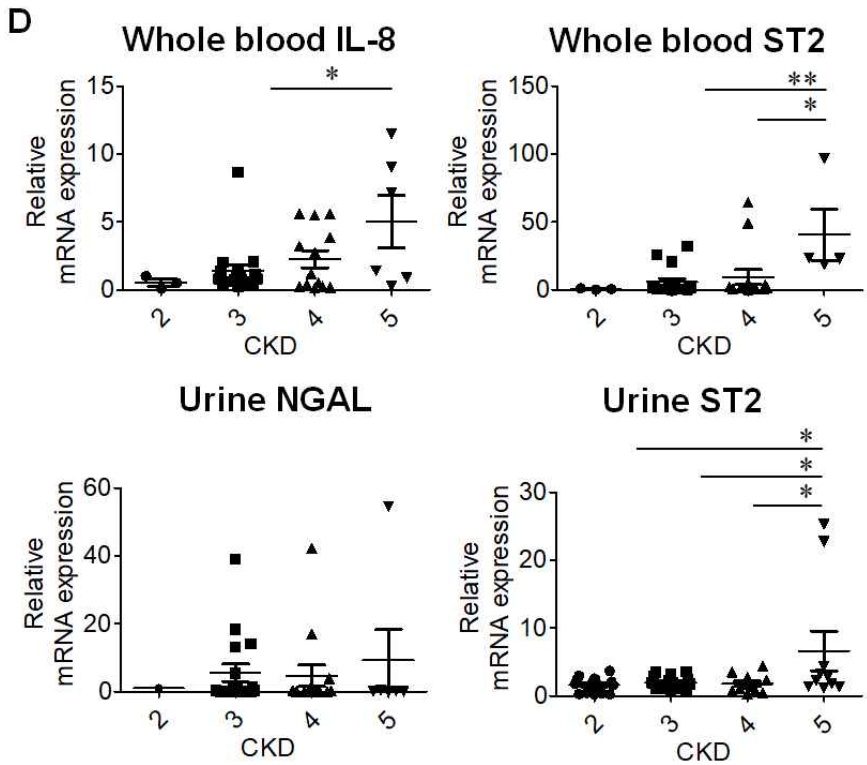

(D) Quantitative RT-PCR analyses of the indicated mRNA transcript in whole blood cells and urine sediment cells from CKD patients.

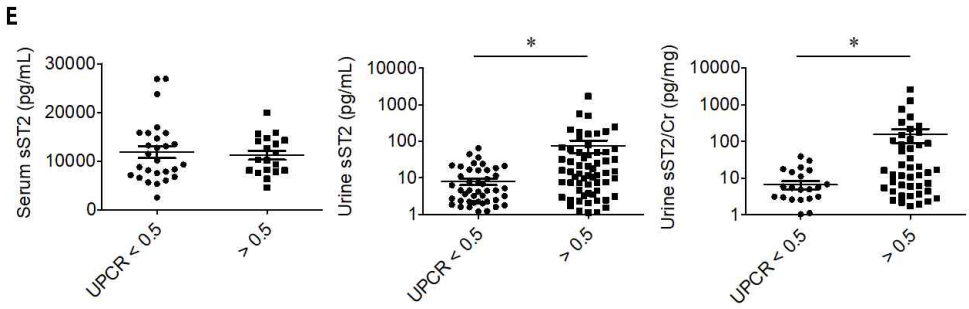

(E) sST2 protein levels in serum and urine of CKD patients stratified by proteinuria (0.5g/g). Symbols represent individual data points, horizontal bars indicate the mean, and error bars indicate SEM (*p < 0.05 , **p < 0.01)

Anti-ST2 therapy modulates fibrosis in podocytes.

We next further examined which are cellular sources of ST2. We thereby performed specific triple immunofluorescence staining of urine sediment cells in CKD patients. As kidney function deteriorates, there were highly detectable ST2-expressing podocytes. The percentage of ST2-expressing podocytes increased as the kidney function deteriorates (Figure 2A) Representative pictures of flow cytometry was showed in Figure 2B. Taken together, ST2-expressing kidney cells, especially podocytes and PTECs, were increased in kidney and urine of patients with reduced kidney function. Therefore we can suggest that they might play a key role in the progression of CKD represented by renal fibrosis.

To assess the role of ST2 in kidney cell fibrosis, we hypothesized that ST2-mediated pathway would aggravate in fibrosis induced kidney cells in vitro experiments. Primary cultured human podocytes were treated with TGF-β to induce fibrosis. Remarkably, the expression of ST2 mRNA was upregulated after TGF-β was introduced ($P < 0.05$), and collagen 1, fibronectin mRNA expression was also increased, showing that fibrosis induction was adequately done (Figure 2C).

We next hypothesized that sST2 blockade would ameliorate podocyte fibrosis. Podocytes treat with TGF-β and anti-ST2 blocking antibody simultaneously displayed significantly down regulated expression of fibronectin and collagen 1 compared with

TGF-β treated podocytes ($P < 0.05$). Western-blot analysis of podocytes further confirmed these findings by showing downregulation of fibronectin after exposure to anti-ST2 mAb (Figure 2D).

Figure 2. Anti-ST2 blockade therapy modulates fibrosis in podocytes.

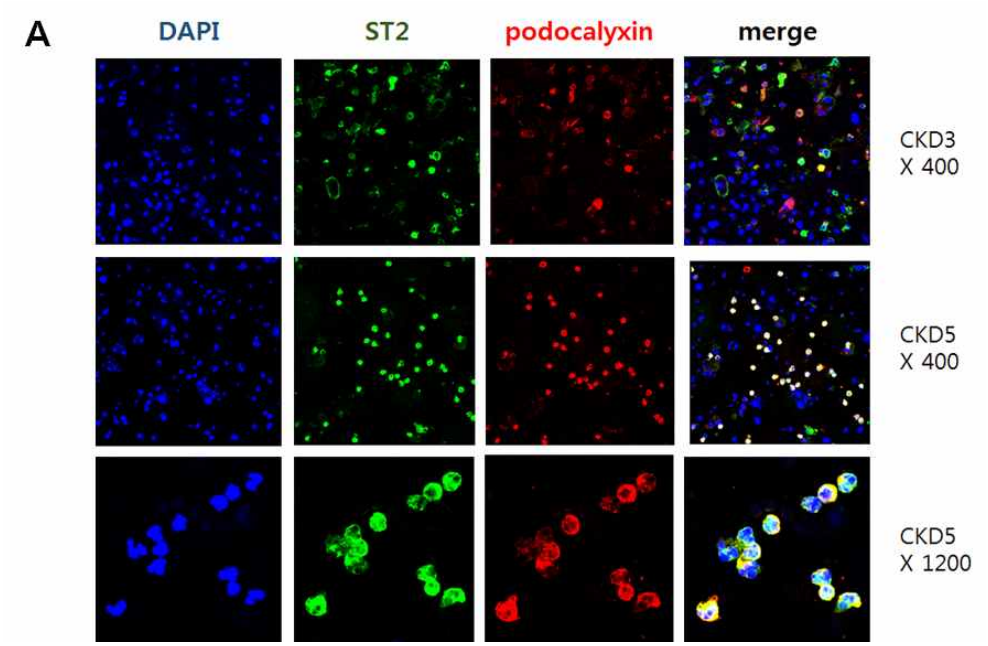

(A) Representative confocal microscopic images of human urine samples in CKD 3 and CKD 5 patients co-stained for ST2L (green), podocalyxin (red) and DAPI (blue). Original magnification: X400 or X1200.

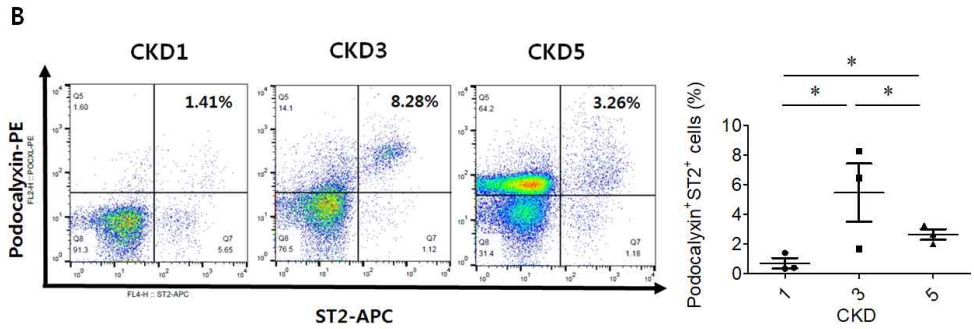

(B) Representative flow cytometic analyses of podocalyxin and ST2 expression in urine sediment cells of CKD patients.

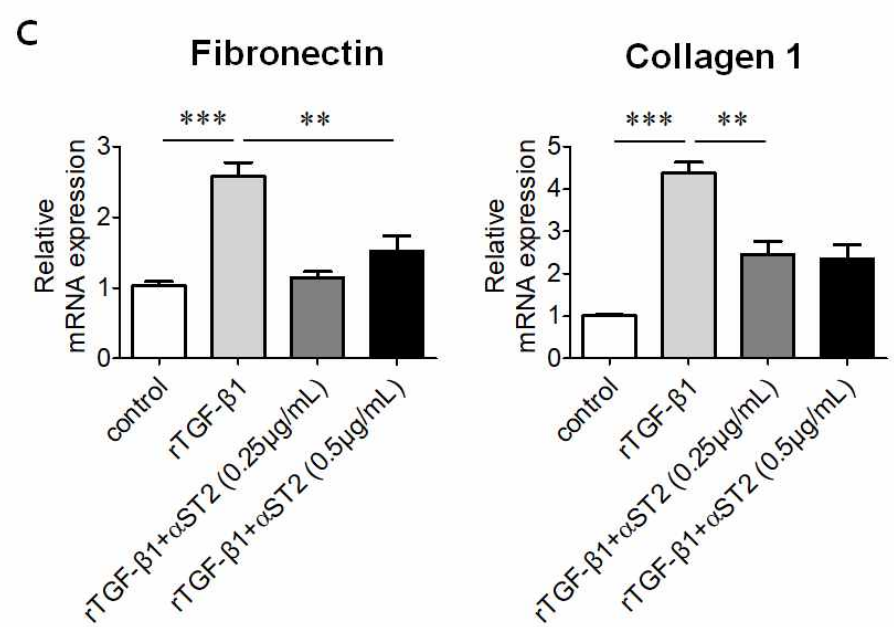

(C) Quantitative RT-PCR analyses of the indicated mRNA transcript in primary cultured podocytes treated with IgG control or αST2 Ab after fibrosis induction with rTGF-β1.

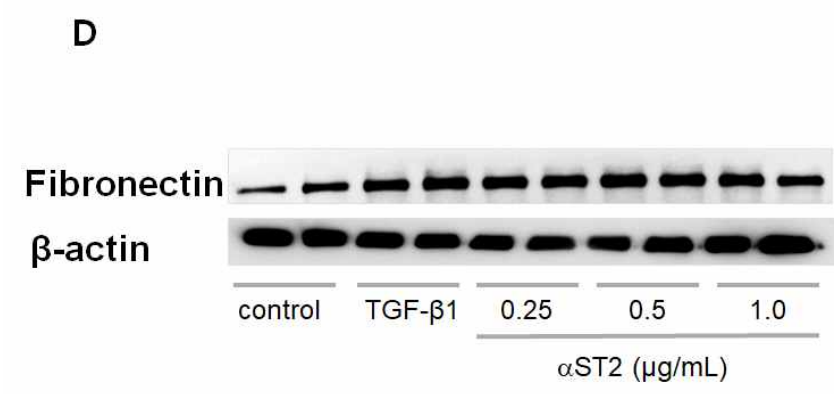

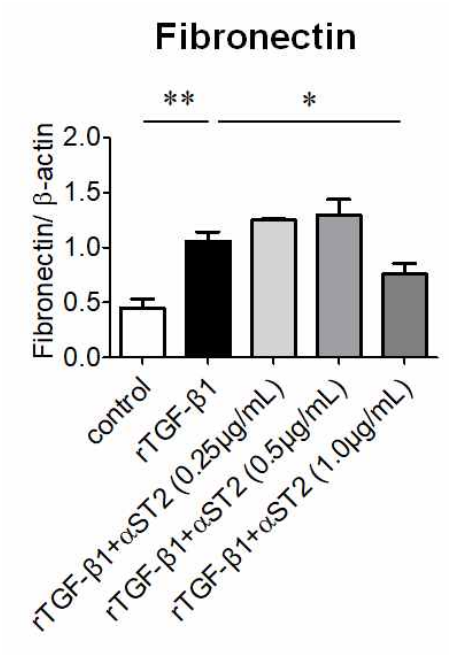

(D) Western blot analysis of IgG control- or αST2 Ab-treated primary cultured podocytes after fibrosis induction with rTGF-β1.

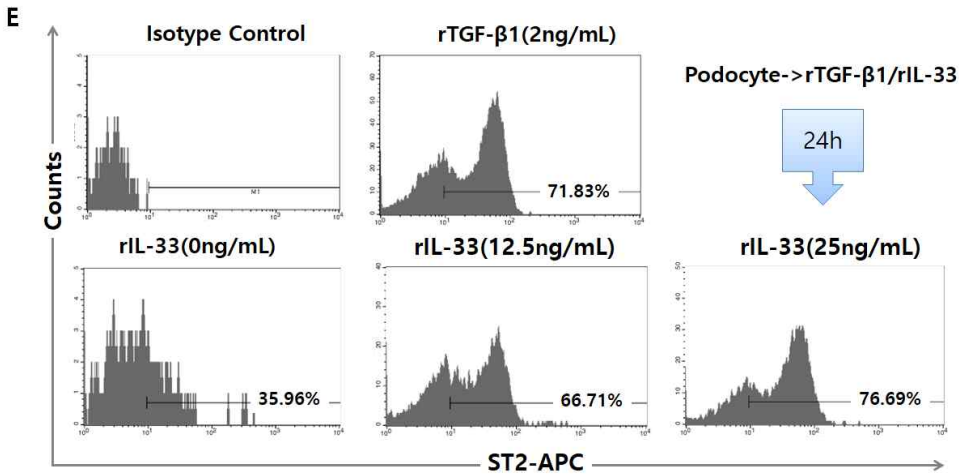

(E) Flow cytometric analyses of ST2 expression on primary cultured podocytes after treating with IgG control, rTGF− β1 and rIL−33. The combined date represent at least 2 independent experiments with similar results. Symbols represent individual data points, horizontal bars indicate the mean, and error bars indicate SEM (*p < 0.05 , **p < 0.01, ***p<0.001)

ST2 blockade prevents rTGF-β1-induced apoptosis in podocytes

The role of ST2 in rTGF-β1-induced apoptosis was investigated in primary cultured human podocyte followed by treatment with or without ST2 blocking Ab (0.5, 1.0 μg/ml). Confocal images and flow cytometric analysis both showed that ST2 blockade consistantly decreased apoptotic cells in dose-dependent manner (Figure 3A, 3B). In confocal images WT-1 expression, which is a key regulator of podocyte function was restored after treating anti-ST2 Ab, and Bcl-2, which is anti-apoptotic regulatory protein also increased after ST2 blockade (Figure 3C-3E). These data indicate that blocking ST2 pathway prevented rTGF-β1-induced apoptosis in podocytes.

Figure 3. Anti-ST2 blockade therapy reduces apoptosis in podocytes.

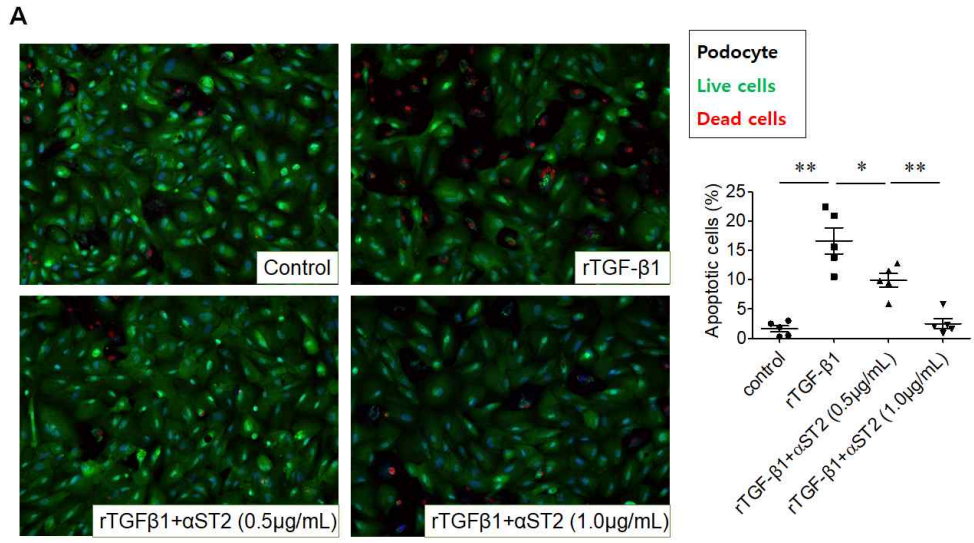

(A) Representative confocal microscopic images for apoptotic cells in IgG control- or αST2-treated primary cultured podocytes after fibrosis induction with rTGF-β1. Apoptotic cells (red), live cells (green). Original magnification: X400.

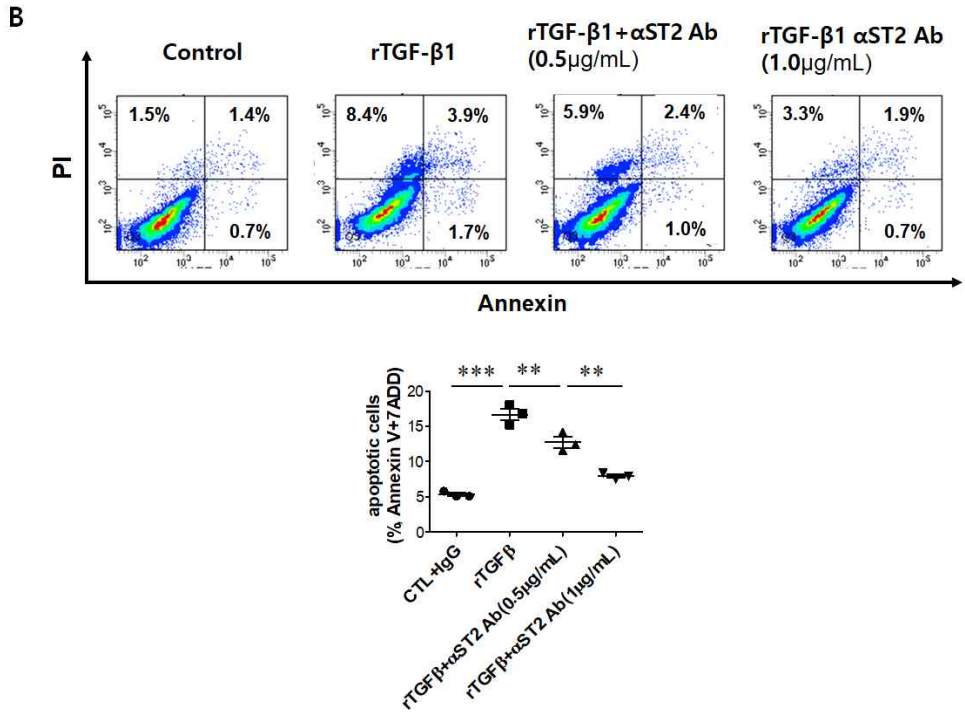

(B) Flow cytometry measurements showed that ST2 blockade attenuated rTGF-β1-induced apoptosis.

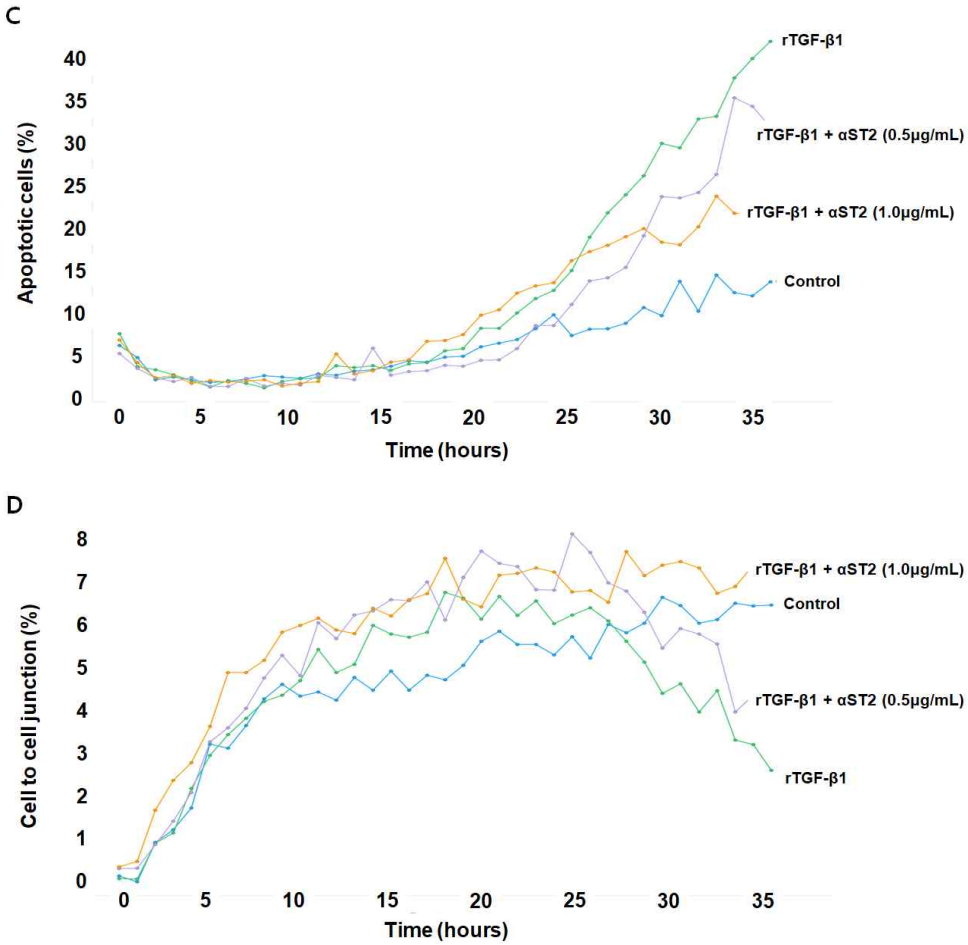

(C, D) Percentage of apoptotic cells, WT-1 positive cells and BCL-2 positive cells.

(E) Representative confocal microscopic images of IgG control-

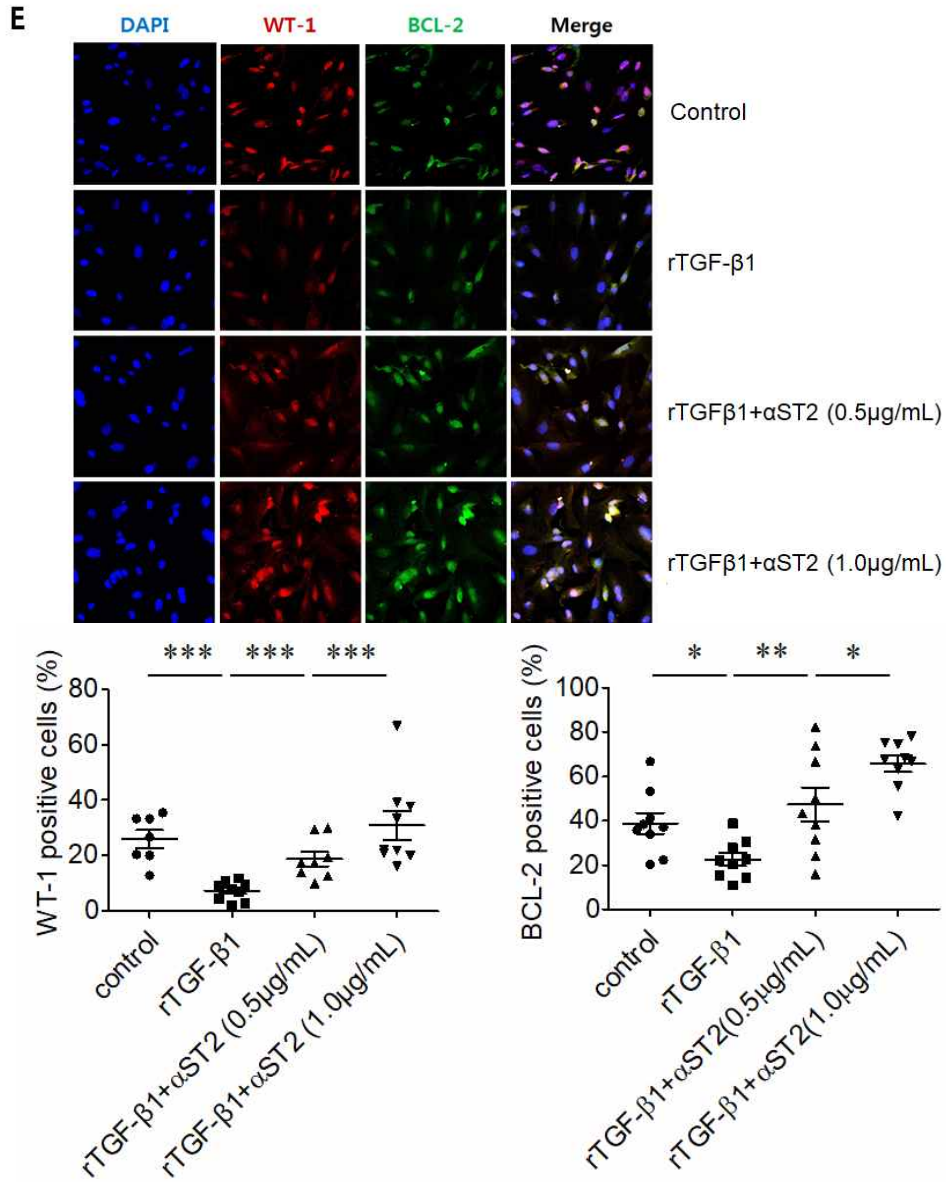

or αST2-treated primary cultured podocytes after fibrosis induction with rTGF-β1 co-stained for WT-1 (red), BCL-2 (green) and DAPI (blue). Original magnification: X400. The combined date represent at least 2 independent experiments with

similar results. Symbols represent individual data points, horizontal bars indicate the mean, and error bars indicate SEM (*p < 0.05 , **p < 0.01, ***p<0.001)

Anti-ST2 blockade therapy ameliorates fibrosis in proximal tubular epithelial cells.

As we showed in IHC-stained kidney specimens of CKD patients, ST2-expressing PTECs were also increased in the urine of CKD III and V patients (Figure 4A). Representative pictures of flow cytometry was showed in Figure 4B. To demonstrate the effect of ST2 on PTECs fibrosis, we performed the same experiment with PTECs. The ST2 was upregulated when fibrosis was induced in PTECs compared with control ($P < 0.01$). On immunoblot of PTECs, there was also an increase in ST2 on TGF-β induced fibrosis compared with control (Figure 4C). We next determined whether neurtralization of the ST2 might also protect in PTECs fibrosis induced by TGF-β. In line with our previous findings, PTECs treat with an anti-ST2 blocking antibody displayed significantly down regulated expression of collagen 1 and αSMA compared with TGF-β treated PTECs ($P < 0.05$) (Figure 4D).

Figure 4. Anti-ST2 blockade therapy ameliorates fibrosis in proximal tubular epithelial cells.

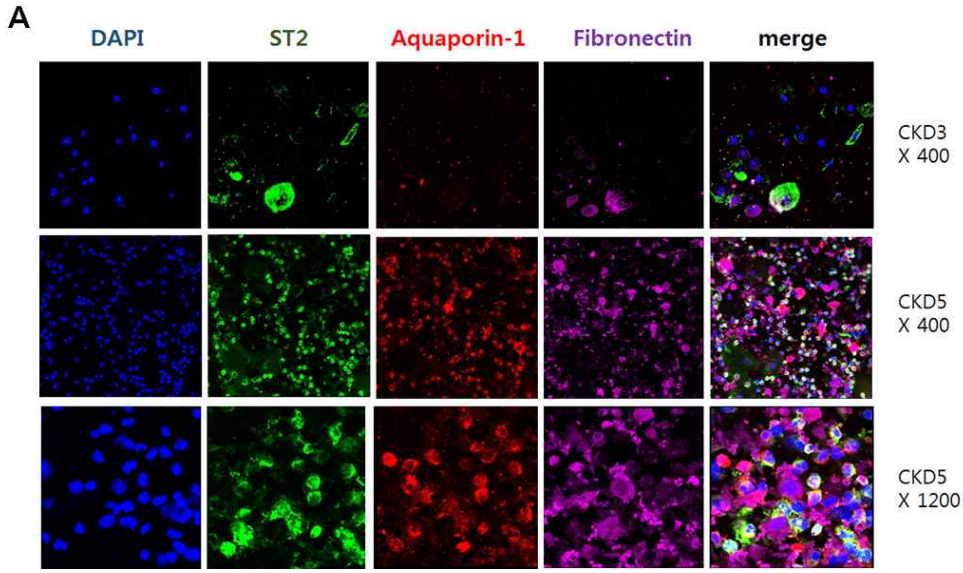

(A) Representative confocal microscopic images of human urine samples in CKD 3 and CKD 5 patients co-stained for ST2L (green), aquaporin-1 (red), fibronectin (purple) and DAPI (blue). Original magnification: X400 or X1200.

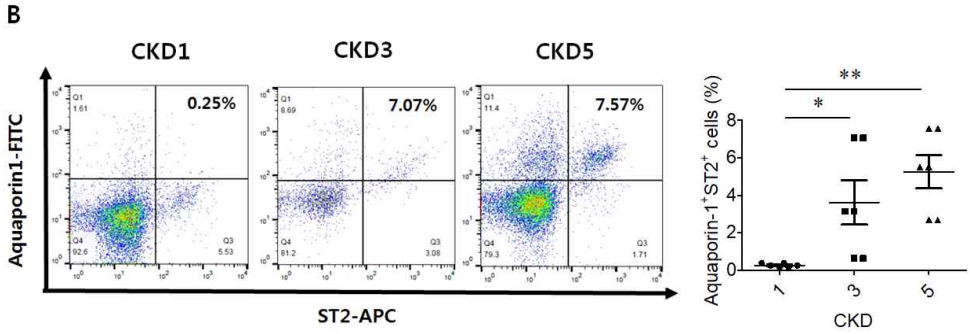

(B) Representative flow cytometic analyses of aquaporin-1 and ST2 expression in urine sediment cells of CKD patients.

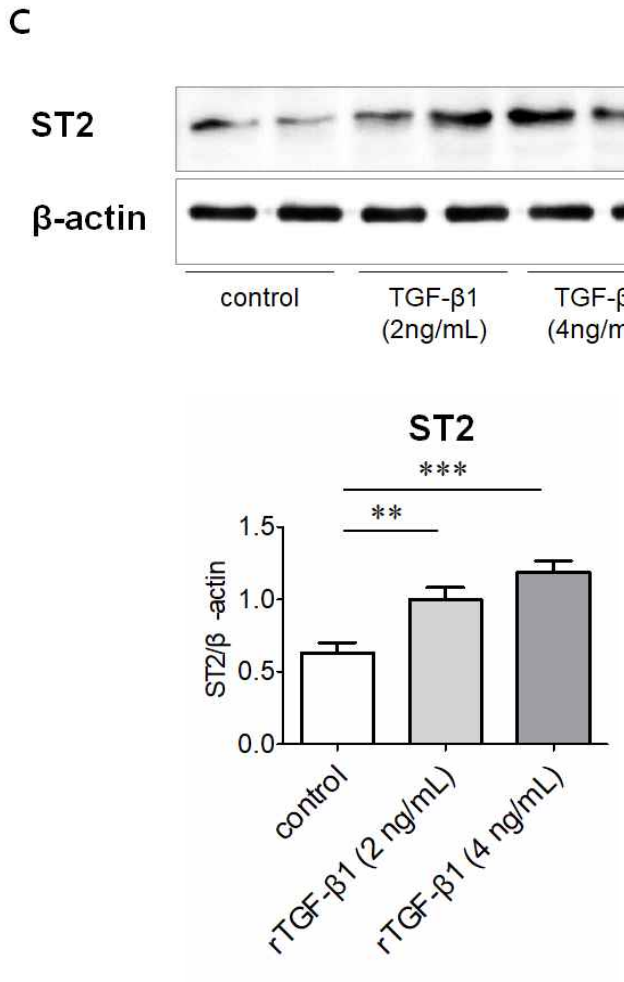

(C) Western blot analysis of IgG control- or rTGF-β1- treated primary cultured PTECs.

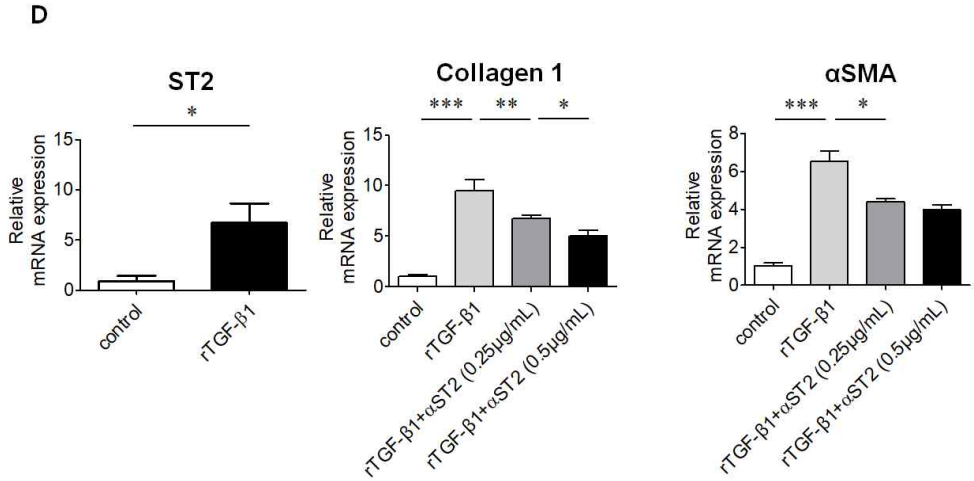

(D) Quantitative RT-PCR analyses of the indicated mRNA transcript in primary cultured proximal tubular epithelial cells (PTECs) treated with IgG control or αST2 after fibrosis induction with rTGF-β1. The combined date represent at least 2 independent experiments with similar results. Symbols represent individual data points, horizontal bars indicate the mean, and error bars indicate SEM (*p < 0.05 , **p < 0.01, ***p<0.001)

ST2 blockade and renal fibrosis in UUO model

We quantitated body weight (bwt) 14 days after unilateral ureteral obstruction (UUO) in mice, bwt decreased after UUO and we observed that anti-ST2 mAb treatment prevented the decrease of bwt (Figure 5A). And we quantitated kidney fibrosis by Masson' s trichrome staining. Two weeks after UUO, renal fibrosis was extensive; however, antiST2-treated UUO mice exhibited reduced renal fibrosis (Figure 5B). To further test the notion that the administration of anti-ST2 mAb would reduce the development of kidney fibrosis, we performed RT-PCR and confocal image analyses. And ST2, fibronectin was decreased after anti-ST2 treatment. (Figure 5C, 5D). In western blot assay, IL-33, Snail, aSMA, b-galactosidase and Bax increased after UUO and this observation prevented as anti-ST2 mAb was treated (Figure 5E, 5F).

Collectively we provided experimental evidence that ST2 contributes to the progression of renal fibrosis in two experimental in vitro models of kidney cell fibrosis, suggesting that pharmacological inhibition of ST2 might represent a novel therapeutic role in renal fibrosis.

Figure 5. ST2 blockade and renal fibrosis in UUO model

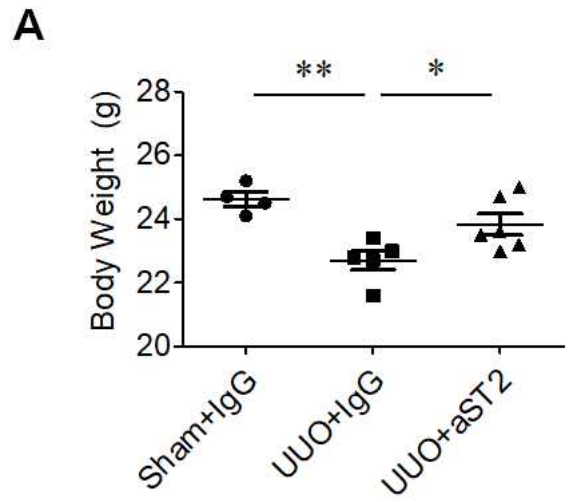

(A) Body weight of IgG control- or αST2-treated mice at day 14 after UUO.

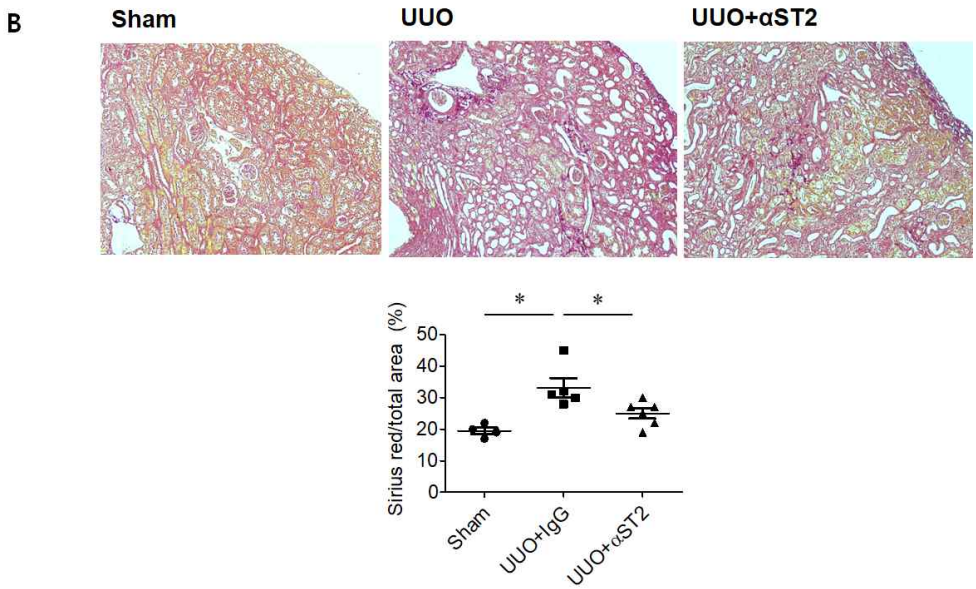

(B) Representative images of kidney sections stained for Sirius red and histologic quantification of percentage of Sirius red positive area over total area in IgG control- or αST2-treated mice at day 14 after UUO.

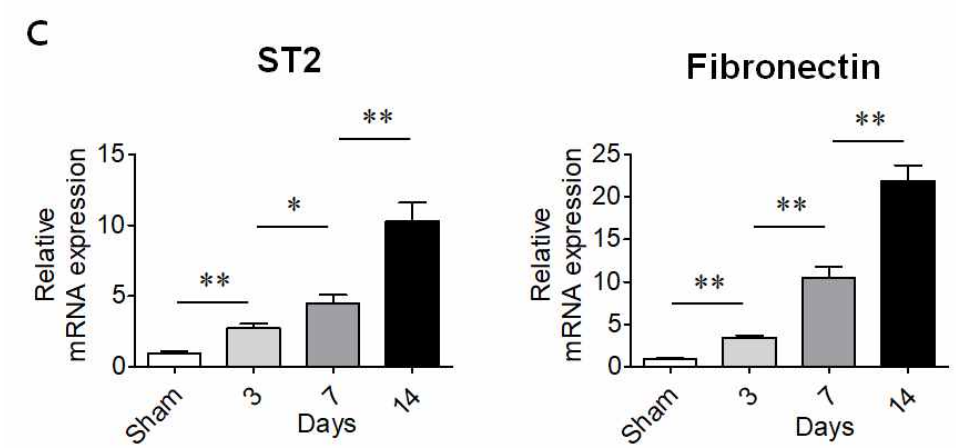

(C) Quantitative RT-PCR analyses of the indicated mRNA transcript.

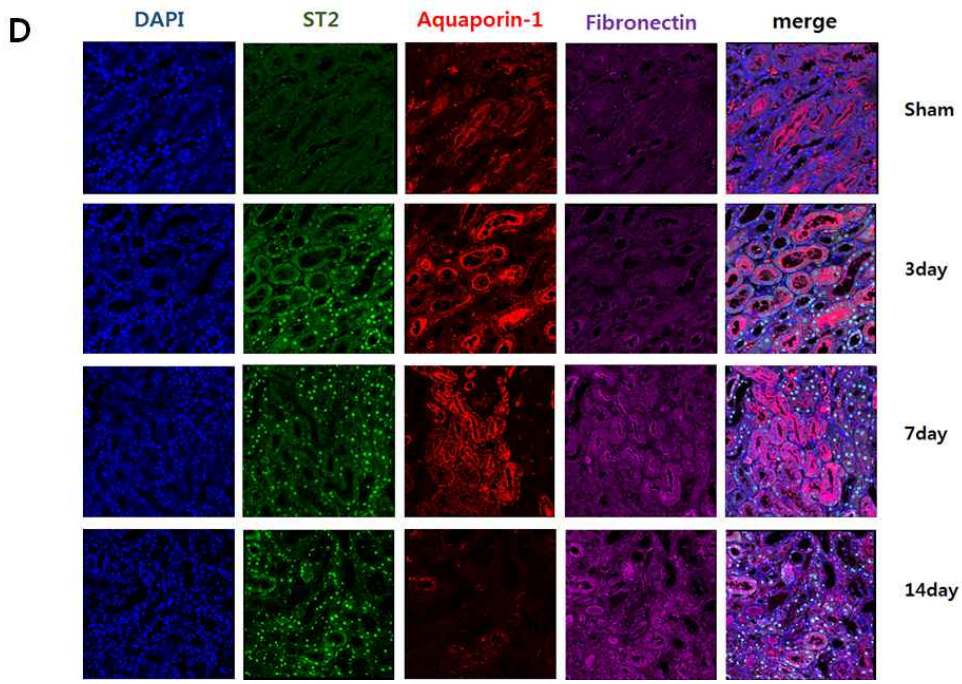
D
DAPI
ST2
Aquaporin-1
Fibronectin
merge
Sham
3day
7day
14day

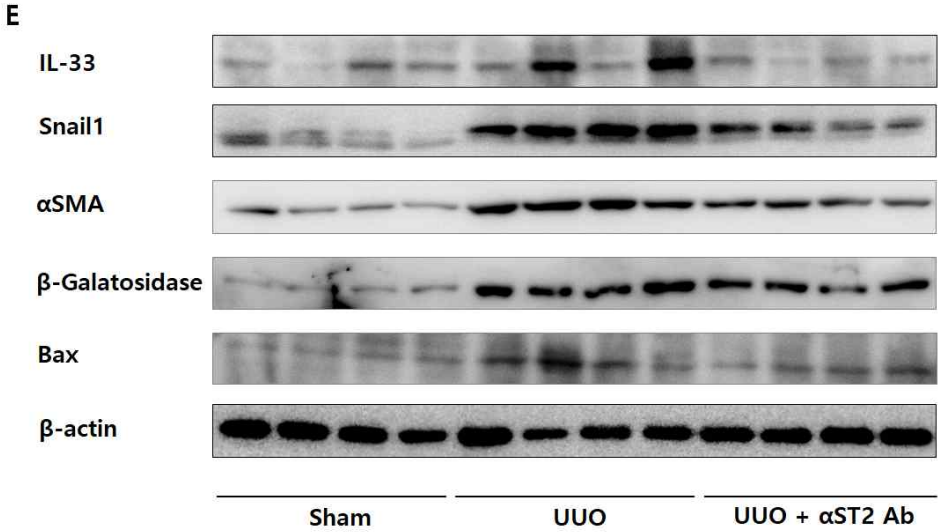
E
IL-33
Snail1
αSMA
β-Galatosidase
Bax
β-actin
Sham
UUO
UUO + αST2 Ab

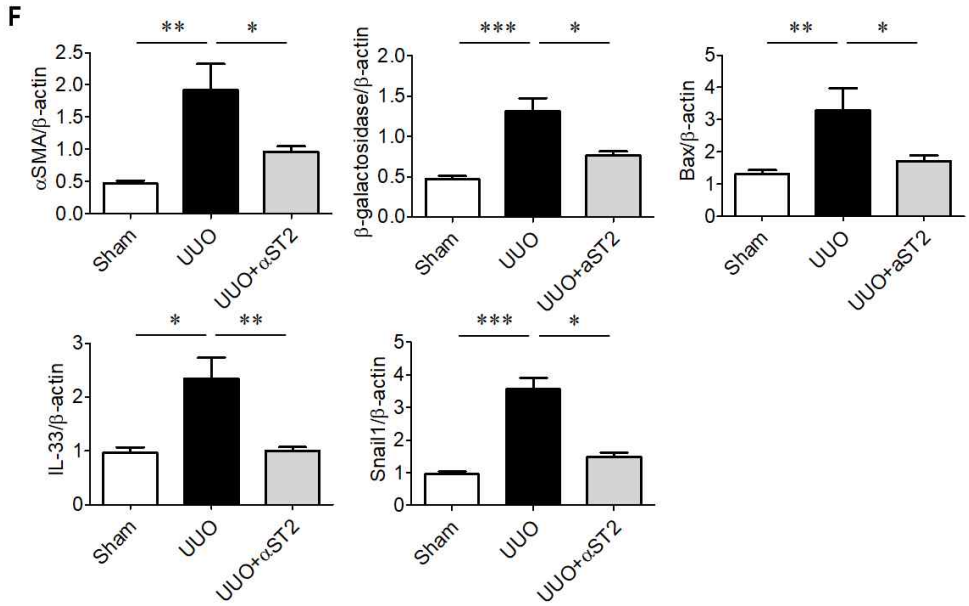

Representative confocal microscopic images (D) and Western blot analysis (E, F) in IgG control- or αST2-treated mice after UUO. UUO, Unilateral-Ureteral Obstruction. The combined date represent at least 2 independent experiments with similar results. Symbols represent individual data points, horizontal bars indicate the mean, and error bars indicate SEM (*p < 0.05 , **p < 0.01, ***p<0.001)

DISCUSSION

This is the first study, to our knowledge, to demonstrate that elevated serum and urine level of sST2 in CKD patients is in correlation with renal function. More importantly, we report that podocytes and PTECs are involved in ST2-related renal fibrosis and inhibition with anti-ST2 mAb ameliorated the progression of fibrosis.

ST2, an IL-1 receptor family member, has known to play a key role in tissue fibrosis in various studies. For example, it has recently been shown that ST2 promotes the initiation and progression of pulmonary fibrosis by recruiting ST2+macrophages and ST2+innate lymphoid cells in mice(17). IL-33/ST2 has also been shown to activate hepatic stellate cell via IL-13 which results in pathologic tissue remodeling and hepatic fibrosis(18). A recent study showed that IL-33/ST2 pathway had a cardioprotective fibroblast-cardiomyocyte paracrine system which is mechanically activated(19).

Renal fibrosis is characterized by glomerulosclerosis and tubulointerstitial fibrosis. Podycytes are recognized to play a key role in the development of kidney fibrosis, especially glomerulosclerosis. Previous studies showed podocytes are involved in mesangial cell and endothelial cell survival and differentiation via vascular endothelial growth factor A (VEGF-A), which is produced by podocytes. Selective loss of

overproduction of VEGF by podocytes results in endothelial cell and mesangial cell dysfunction and progressive glomerulosclerosis (6, 7, 20). Moreover, recent data demonstrated podocyte-induced epithelial-mesenchymal transition (EMT) which is induced by TGF-β1, also contributes to the development of kidney fibrosis(8). The observation that podocytes undergo EMT suggests an incredible plasticity of these terminally differentiated cells in certain pathological conditions. Given that podocyte and tubular epithelial cells are developmentally derived from the same origin, it comes as little surprise that podocytes, similar to tubular epithelial cells, undergo a phenotypic conversion after TGF-β1 stimulation(8).

On the other hand, tubular EMT is a, well known, pathogenic mechanism that occurs in the fibrotic tissue after recurrent chronic injury which results in tubulointerstitial fibrosis(21, 22).

It is widely accepted that transforming growth factor-b (TGF-β) and its downstream Smad signaling play an essential role. The importance of TGF-β in tissue fibrosis in general, and renal fibrosis in particular.

Upregulation of TGF-β is a universal finding in virtually every type of CKD, both in animal models and in humans. In vitro, TGF-β as a sole factor can stimulate mesangial cells, interstitial fibroblasts, and tubular epithelial cells to undergo myofibroblastic activation or transition, to become matrix-producing fibrogenic cells.

In the present study, ST2 expression was increased after TGF-β induction in both primary cultured podocytes and PTECs. Furthermore, after ST2 blockade, fibrosis was neutralized in both podocytes and PTECs. Collectively we propose that ST2 is involved in renal fibrosis in both podocytes and PTECs. And the findings reported here strongly suggest a mechanism of both glomerulosclerosis and tubulointerstitial fibrosis. During this mechanism ST2 might play a key role to these two types of kidney cells.

Inflammation and fibrosis often occur simultaneously in CKD, suggesting that both are associated with disease progression (23,24). However, molecular mechanisms linking these activities have not been fully clarified. Many reports indicate that TGF-β plays a pivotal role in the development of fibrosis, and also SNAIL, which is a transcriptional factor, is a potent inducer of renal fibrosis (25). Recent reports suggest that renal fibrosis, especially tubular epithelial cells might be regulated by signaling upstream of SNAIL (26). We demonstrated in UUO model that SNAIL expression was increased after fibrosis induction, and ST2 blockade prevented not only the expression of SNAIL, but also the protein expressions of fibrosis markers such as αSMA.

It is well known that excessive apoptosis promotes fibrosis and organ dysfunction (27,28), and there are evidence for an apparent interplay between early apoptosis and subsequent fibrosis, and the apoptosis could be an early event that occurs

before the onset of fibrosis (29-31). We showed that in primary cultured human podocytes, exposure to anti-ST2 Ab prevented TGF-β induced apoptosis and fibrosis, respectively. In UUO mouse model, ST2 blockade significantly attenuated the protein expression of Bax and αSMA, simultaneously. Taken together, our data indicate that ST2 blockade ameliorates renal fibrosis by inhibiting both renal podocyte apoptosis and TIF.

In this study, we evaluated serum and urine sST2 levels in CKD patients and found that increased levels of sST2 is related with the process of renal fibrosis. However, there was no data with in vivo animal CKD models. Further investigation are required to figure out the mechanisms and the exact effects in renal fibrosis.

Kidney is composed of various kinds of cells such as vascular endothelial cells, mesangial cells, podocytes, tubular cells, fibroblasts and stromal cells. Renal fibrosis is a complex histopathological process which clearly necessitates the participation and interaction of many types of kidney resident and infiltrated cells (32,33). Therefore, further studies to explore the role of other renal cells and the interactions between these cells in ST2-mediated renal fibrosis.

In summary, our findings demonstrated podocytes and PTECs is considerably related in ST2-mediated renal fibrosis that can be blocked with anti-ST2 mAb. And we suggest that ST2 blockage offers new perspectives on a novel therapeutic target to prevent

and treat renal fibrosis in CKD patients.

REFERENCES

1. Saran R, Li Y, Robinson B, Abbott KC, Agodoa LY, Ayanian J, et al. US Renal Data System 2015 Annual Data Report: Epidemiology of Kidney Disease in the United States. Am J Kidney Dis. 2016;67(3 Suppl 1):Svii, S1-305.

2. Bohle A, Mackensen-Haen S, von Gise H. Significance of tubulointerstitial changes in the renal cortex for the excretory function and concentration ability of the kidney: a morphometric contribution. Am J Nephrol. 1987;7(6):421-33.

3. Wynn TA. Common and unique mechanisms regulate fibrosis in various fibroproliferative diseases. J Clin Invest. 2007;117(3):524-9.

4. Nangaku M. Chronic hypoxia and tubulointerstitial injury: a final common pathway to end-stage renal failure. J Am Soc Nephrol. 2006;17(1):17-25.

5. Liu Y. Renal fibrosis: new insights into the pathogenesis and therapeutics. Kidney Int. 2006;69(2):213-7.

6. Eremina V, Baelde HJ, Quaggin SE. Role of the VEGF--a signaling pathway in the glomerulus: evidence for crosstalk between components of the glomerular filtration barrier. Nephron Physiol. 2007;106(2):p32-7.

7. Eremina V, Cui S, Gerber H, Ferrara N, Haigh J, Nagy A, et al. Vascular endothelial growth factor a signaling in the podocyte-endothelial compartment is required for mesangial cell migration and survival. J Am Soc Nephrol. 2006;17(3):724-35.

8. Li Y, Kang YS, Dai C, Kiss LP, Wen X, Liu Y. Epithelial-to-mesenchymal transition is a potential pathway leading to podocyte dysfunction and proteinuria. Am J Pathol. 2008;172(2):299-308.

9. Yu SL, Wong CK, Tam LS. The alarmin functions of high-mobility group box-1 and IL-33 in the pathogenesis of systemic lupus erythematosus. Expert Rev Clin Immunol. 2013;9(8):739-49.

10. Yang F, Zhu P, Duan L, Yang L, Wang J. IL33 and kidney disease (Review). Mol Med Rep. 2016;13(1):3-8.

11. Schmitz J, Owyang A, Oldham E, Song Y, Murphy E, McClanahan TK, et al. IL-33, an interleukin-1-like cytokine that signals via the IL-1 receptor-related protein ST2 and induces T helper type 2-associated cytokines. Immunity. 2005;23(5):479-90.

12. Mok MY, Huang FP, Ip WK, Lo Y, Wong FY, Chan EY, et al. Serum levels of IL-33 and soluble ST2 and their association with disease activity in systemic lupus erythematosus. Rheumatology (Oxford). 2010;49(3):520-7.

13. Thierry A, Giraud S, Robin A, Barra A, Bridoux F, Ameteau V, et al. The alarmin concept applied to human renal transplantation: evidence for a differential implication of HMGB1 and IL-33. PLoS One. 2014;9(2):e88742.

14. Bao YS, Na SP, Zhang P, Jia XB, Liu RC, Yu CY, et al. Characterization of interleukin-33 and soluble ST2 in serum and

their association with disease severity in patients with chronic kidney disease. J Clin Immunol. 2012;32(3):587-94.

15. Mundel P, Reiser J, Kriz W. Induction of differentiation in cultured rat and human podocytes. J Am Soc Nephrol. 1997;8(5):697-705.

16. Shankland SJ, Pippin JW, Reiser J, Mundel P. Podocytes in culture: past, present, and future. Kidney Int. 2007;72(1):26-36.

17. Fadok VA, Voelker DR, Campbell PA, Cohen JJ, Bratton DL, Henson PM. Exposure of phosphatidylserine on the surface of apoptotic lymphocytes triggers specific recognition and removal by macrophages. J Immunol. 1992;148(7):2207-16.

18. Kavitha CV, Nambiar M, Ananda Kumar CS, Choudhary B, Muniyappa K, Rangappa KS, et al. Novel derivatives of spirohydantoin induce growth inhibition followed by apoptosis in leukemia cells. Biochem Pharmacol. 2009;77(3):348-63.

19. Zamai L, Falcieri E, Marhefka G, Vitale M. Supravital exposure to propidium iodide identifies apoptotic cells in the absence of nucleosomal DNA fragmentation. Cytometry. 1996;23(4):303-11.

20. Li D, Guabiraba R, Besnard AG, Komai-Koma M, Jabir MS, Zhang L, et al. IL-33 promotes ST2-dependent lung fibrosis by the induction of alternatively activated macrophages and innate lymphoid cells in mice. J Allergy Clin Immunol. 2014;134(6):1422-32 e11.

21. McHedlidze T, Waldner M, Zopf S, Walker J, Rankin AL, Schuchmann M, et al. Interleukin-33-dependent innate lymphoid cells mediate hepatic fibrosis. Immunity. 2013;39(2):357-71.
22. Sanada S, Hakuno D, Higgins LJ, Schreiter ER, McKenzie AN, Lee RT. IL-33 and ST2 comprise a critical biomechanically induced and cardioprotective signaling system. J Clin Invest. 2007;117(6):1538-49.
23. Eremina V, Jefferson JA, Kowalewska J, Hochster H, Haas M, Weisstuch J, et al. VEGF inhibition and renal thrombotic microangiopathy. N Engl J Med. 2008;358(11):1129-36.
24. Liu Y. Epithelial to mesenchymal transition in renal fibrogenesis: pathologic significance, molecular mechanism, and therapeutic intervention. J Am Soc Nephrol. 2004;15(1):1-12.
25. Kalluri R, Neilson EG. Epithelial-mesenchymal transition and its implications for fibrosis. J Clin Invest. 2003;112(12):1776-84.
26. Lamouille S, Xu J, Derynck R. Molecular mechanisms of epithelial-mesenchymal transition. Nat Rev Mol Cell Biol. 2014;15(3):178-96.
27. Xu J, Lamouille S, Derynck R. TGF-beta-induced epithelial to mesenchymal transition. Cell Res. 2009;19(2):156-72.
28. Lovisa S, LeBleu VS, Tampe B, Sugimoto H, Vadnagara K, Carstens JL, et al. Epithelial-to-mesenchymal transition induces cell cycle arrest and parenchymal damage in renal

fibrosis. Nat Med. 2015;21(9):998-1009.

29. Simon-Tillaux N, Hertig A. Snail and kidney fibrosis. Nephrol Dial Transplant. 2017;32(2):224-33.

30. Mao H, Li Z, Zhou Y, Li Z, Zhuang S, An X, et al. HSP72 attenuates renal tubular cell apoptosis and interstitial fibrosis in obstructive nephropathy. Am J Physiol Renal Physiol. 2008;295(1):F202-14.

31. Kim J, Kim DS, Park MJ, Cho HJ, Zervos AS, Bonventre JV, et al. Omi/HtrA2 protease is associated with tubular cell apoptosis and fibrosis induced by unilateral ureteral obstruction. Am J Physiol Renal Physiol. 2010;298(6):F1332-40.

32. Havasi A, Borkan SC. Apoptosis and acute kidney injury. Kidney Int. 2011;80(1):29-40.

33. Johnson A, DiPietro LA. Apoptosis and angiogenesis: an evolving mechanism for fibrosis. FASEB J. 2013;27(10):3893-901.

34. Huang Y, Sun Y, Cao Y, Sun H, Li M, You H, et al. HRD1 prevents apoptosis in renal tubular epithelial cells by mediating eIF2alpha ubiquitylation and degradation. Cell Death Dis. 2017;8(12):3202.

35. Liu Y. Cellular and molecular mechanisms of renal fibrosis. Nat Rev Nephrol. 2011;7(12):684-96.

36. Boor P, Ostendorf T, Floege J. Renal fibrosis: novel insights into mechanisms and therapeutic targets. Nat Rev Nephrol. 2010;6(11):643-56.

국문 초록

IL-33의 수용체인 Suppression of tumorigenicity 2 (ST2)는 신손상이 발생하였을 때 신조직을 보호하고 재생하는데 중요한 역할을 하는 것으로 알려져 있다. 본 연구에서는 신장섬유화 과정에서 ST2를 차단하는 것이 신장섬유화에 미치는 영향 및 기전에 대해 보고하고자 한다.

본 연구에서는 296명의 만성콩팥병 환자에서 혈청 및 소변의 sST2 농도를 측정하였다. 말초혈액 및 소변에서 ST2 mRNA 농도를 측정하였고, 면역형광염색을 통해 만성콩팥병 신장 환자들에서 ST2의 존재여부를 확인하였다. 소변세포를 분리하여 podocalyxin/aquaporin-1 및 ST2를 동시에 염색하여 이러한 소변 세포의 종류를 확인하였다. 초대배양한 인체 족세포 및 근위세뇨관세포에서 TGF-β를 통해 섬유화를 유도하였고, 이후에 ST2 monoclonal Ab를 처리하여 신장섬유화가 호전되는지를 평가하였다. 마지막으로 만성콩팥병 동물모델(UUO)에서 ST2 및 섬유화 표지자를 확인하고, ST2 Ab를 처리하였을 때 섬유화 호전여부를 평가하였다.

sST2 농도는 만성콩팥병 환자의 신기능이 감소함에 따라 혈청(P=0.023)과 소변(P<0.001)에서 감소하였다. 단백뇨 0.5g/g을 기준으로 나누었을 때 단백뇨가 많은 환자들에서 소변 sST2 농도가 통계적으로 높은 것을 확인하였다 (P=0.02). 만성콩팥병 환자들의 소변에서 신기능이 감소함에 따라 ST2가 발현된 신장 족세포 및 근위 세뇨관 세포

의 비율은 증가하였다. 신장 족세포 및 근위 세뇨관 세포에 섬유화를 유발시키면 ST2 발현이 증가하는 것을 확인하였고, ST2 차단 항체를 처리하였을 때 이러한 섬유화는 호전되었다. UUO 만성콩팥병 동물모델에서 ST2 차단 항체를 투여하였을 때 fibronectin 등의 섬유화 표지자가 감소하는 것을 확인하였다 ($P<0.01$).

만성 콩팥병이 진행함에따라 혈청 및 소변 sST2의 농도는 증가하고, 이러한 과정에는 신장 족세포 및 근위세뇨관 세포가 관여한다. ST2매개 신호체계는 신장섬유화 과정에 상당한 역할을 할 것으로 예상되고, ST2 차단 항체는 신장기능을 보호하는 중요한 치료제가 될 수 있겠다.

주요어: ST2, 신장 족세포, 근위 세뇨관 세포, 만성 콩팥병, 신장 섬유화.

학번: 2010-21888